

Indian Journal of Chemistry
Vol. 59A, July 2020, pp. 923-928

Luminescence quenching of tris(4,4'-dimethyl-2,2'-bipyridyl)ruthenium(II) complex with quinones in aprotic polar medium

T Sumitha Celin & G Allen Gnana Raj*

Department of Chemistry & Research Centre, Scott Christian College (Autonomous), Nagercoil, Tamilnadu, India
E-mail: allengraj@gmail.com*Received 10 January 2020; revised and accepted 19 May 2020*

The photoinduced electron transfer interaction between a luminescent metal-ligand probe, $[\text{Ru}(\text{dmbpy})_3]^{2+}$ and quinones have been investigated by absorption and fluorescence spectroscopy. The reactions of quinones with the excited state ruthenium(II) complex in DMF have been studied by luminescence quenching technique and the bimolecular quenching rate constant k_q values are found close to the diffusion controlled rate. The complex has an absorption maximum of 458 nm. It shows a photoluminescence at 608 nm. The lifetime of the complex in DMF is 164 ns. The ground state absorption measurements are used to confirm the nature of quenching. Transient absorption spectral measurements are performed and the oxidative nature of quenching is confirmed. The detection of semiquinone anion radical using time resolved transient absorption spectroscopy and the linear variation of $\log k_q$ vs reduction potential of the quinones confirms the electron transfer nature of the reaction.

Keywords: Quinones, luminescence, Stern-Volmer equation, Static quenching, Transient absorption spectra

Quinones are ubiquitous in nature. *p*-quinones are important molecules in electron transport. They are electron acceptors in photosynthesis¹⁻³. Photosynthesis occurs through a series of photoinduced electron transfer reactions that convert solar energy to chemical energy in the chloroplast of green plants. Their redox behavior plays a vital role in electrochemical reactions during biological energy transduction and storage. Biological respiration also occurs through multiple redox reactions involving quinone species. The study of electron transfer reaction from quinones (donor) to an acceptor (d^6) metal complex is of great interest. The present study concentrates on the photoinduced electron transfer reaction of $[\text{Ru}(\text{dmbpy})_3]^{2+}$ with quinones in dimethyl formamide (DMF).

Ruthenium(II) complexes have been extensively studied as a promising functional molecule because of their unique photophysical and photochemical as well as related to the photoexcited triplet metal-to-ligand charge transfer (MLCT³) state. The redox properties include electrochromism, proton-coupled electron transfer and multi electron catalysis. These properties are responsible for the potential applications of polypyridyl ruthenium(II) complexes to a large variety of devices including sensors, displays, photocatalysts and in artificial photosynthesis⁴⁻¹¹. The

excited state properties of $[\text{Ru}(\text{NN})_3]^{2+}$ complexes are dramatically affected by the introduction of electron donating and electron withdrawing substituents in 4,4'-position of 2,2'-bipyridine. This long lived excited states exhibit an emission and therefore photoinduced energy/electron transfer can be probed by luminescence technique. Luminescence quenching is associated with variety of molecular interactions like excited state reactions, molecular rearrangements, energy transfer, collisional (or dynamic) quenching and ground state complex formation (or static quenching)¹².

Materials and Methods

$[\text{Ru}(\text{dmbpy})_3]^{2+}$ complex was synthesized by known procedure¹³. The quinones used in this study were obtained from Sigma Aldrich and were used as such. DMF solvent was procured from Merck and used as received. $\text{RuCl}_3 \cdot 3\text{H}_2\text{O}$ and 4,4'-dimethyl-2,2'-bipyridine complexes were dissolved in 20 ml of ethylene glycol and cooled at room temperature and filtered to remove the insoluble impurities. A saturated solution of sodium tetrafluoroborate was then added dropwise into the filtrate until an orange precipitate was formed. The product was filtered, washed with cold water and diethyl ether and further dried in vacuum desiccator. The resultant complex was characterized by UV, IR, ¹H NMR spectra.

Absorption spectral studies

Sample solutions of $[\text{Ru}(\text{dmbpy})_3]^{2+}$ and quinones were freshly prepared for each measurement in DMF solvent. The concentration of $[\text{Ru}(\text{dmbpy})_3]^{2+}$ was taken as 2×10^{-5} M and the quinone concentration was varied between 4×10^{-5} M and 2.8×10^{-4} M. Absorption spectrum was recorded using SYSTRONICS 2203 Double beam UV visible spectrophotometer.

Emission studies and excited state lifetime measurement

Emission spectral measurement was carried out using JASCO FP 8600 spectrofluorometer. The sample solutions were deaerated for 30 min using dry N_2 gas purging by keeping the solution in cold water, to ensure that there is no change in the volume of the solution. Both absorption and emission studies were carried out using samples of same concentration.

Excited state lifetime and transient absorption measurements were made with laser flash photolysis technique using an applied photophysics SP-Quanta Ray GCR-2(10) Nd:YAG laser as the excitation source¹⁴. The lifetime of the complex in DMF is 164 ns. The time dependence of the luminescence was observed using a Czerny-Turner monochromator with a stepper motor control and a Hamamatsu R-928 photomultiplier tube. The production of the excited state on exposure to 355 nm was measured by monitoring the absorbance change. Transient spectra were obtained by a point to point technique, monitoring the change in absorbance (ΔA) after the flash at intervals of 10 nm over the spectral range of 300–800 nm averaging at least 30 decays at each wavelength. Electrochemical measurements were performed using CH16005E electrochemical workstation at room temperature. Cyclic voltammetry measurements were carried out for 10^{-3} M sample solution in DMF consisting of 0.1 M tetrabutylammonium perchlorate supporting electrolyte with a conventional three electrode system containing a platinum working electrode (2 mm diameter), a platinum wire counter electrode and a non-aqueous Ag/AgCl reference electrode. Cyclic voltammograms were recorded after the solutions are purged with N_2 gas for 30 min prior to use.

Results and Discussion

$[\text{Ru}(\text{dmbpy})_2]^{2+}$ complex was synthesized as given in the experimental section. The structure of the quinones and the complex used in the present study are shown in Fig. 1 and 2.

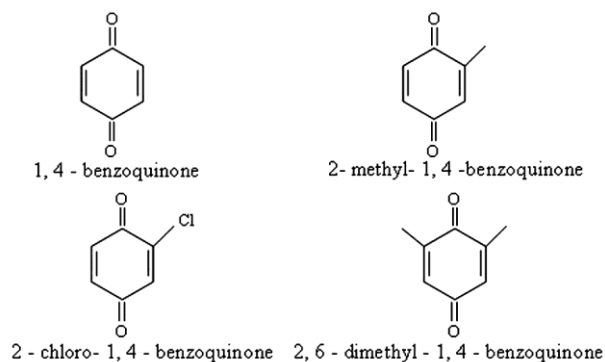


Fig. 1 — Structure of the quinones.

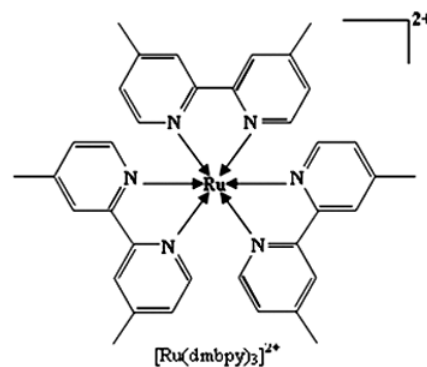


Fig. 2 — Structure of the complex used for the present study.

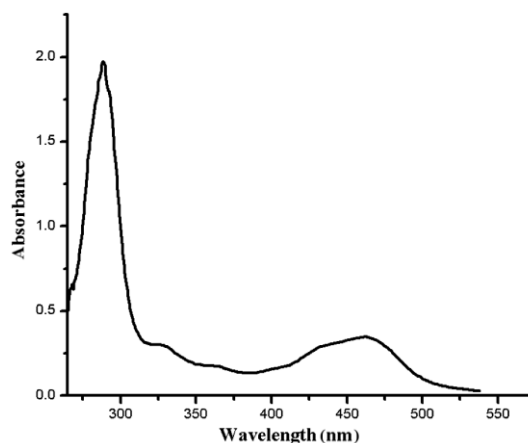


Fig. 3 — Absorption spectrum of $[\text{Ru}(\text{dmbpy})_3]^{2+}$ in DMF.

Steady state absorption and emission properties of $[\text{Ru}(\text{dmbpy})_3]^{2+}$

$[\text{Ru}(\text{dmbpy})_3]^{2+}$ has an absorption maximum at 458 nm (Fig. 3) and The bands at 285 nm is due to the $\pi \rightarrow \pi^*$ transition. The two intense bands at 287 nm and 458 nm have been assigned to MLCT $d \rightarrow \pi^*$ transition. The photophysical properties of $[\text{Ru}(\text{dmbpy})_3]^{2+}$ arise from the population of MLCT state. It has an emission maximum of 608 nm in

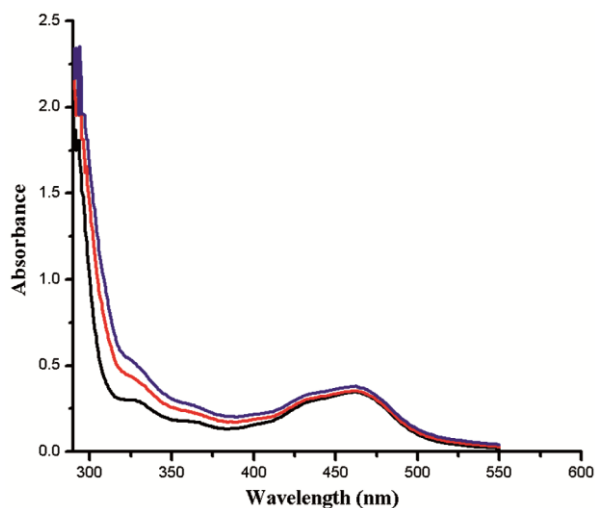


Fig. 4 — Absorption spectrum of $[\text{Ru}(\text{dmbpy})_3]^{2+}$ with incremental concentration of 1,4-benzoquinone in DMF.

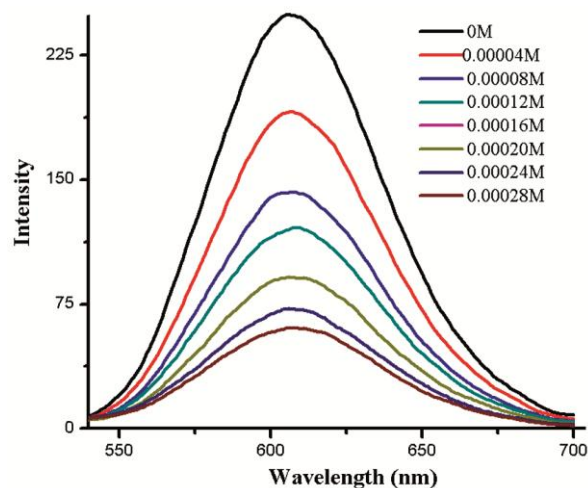


Fig. 5 — Emission spectrum of $[\text{Ru}(\text{dmbpy})_3]^{2+}$ with incremental addition of 2-methyl-1,4-benzoquinone in DMF.

DMF. The absorption spectrum of $[\text{Ru}(\text{dmbpy})_3]^{2+}$ with incremental concentration of 1,4-benzoquinone in DMF is displayed in Fig. 4. There is a steady increase in the MLCT absorption maximum, indicates the formation of ground state complex. The ground state absorption studies of the complex with quinones confirm the static nature of quenching. The binding of the complex with the quencher is due to the $\pi - \pi$ stacking interactions. Thus the absorption spectrum shows the predominance of static quenching. The emission spectrum of $[\text{Ru}(\text{dmbpy})_3]^{2+}$ with incremental addition of quinones is shown in Fig. 5. The emission maximum of Ru(II) complexes originate from the $d_{\pi-\pi^*}$ MLCT³ transition.

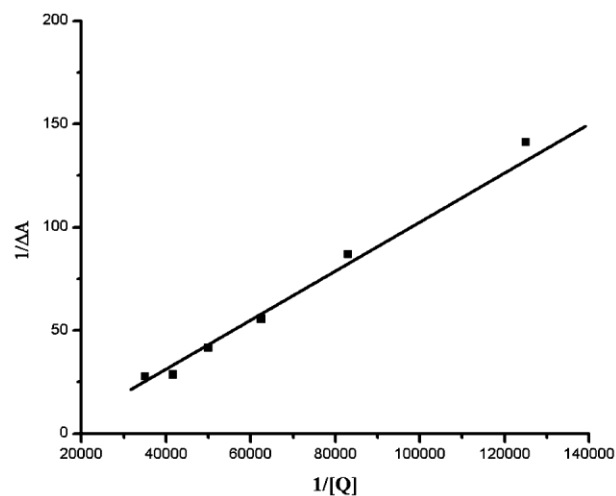


Fig. 6 — Benesi-Hildebrand plots from the luminescence quenching data of $*[\text{Ru}(\text{dmbpy})_3]^{2+}$ with incremental addition of 2-chloro-1,4-benzoquinone in DMF.

Table 1 — Binding constant and first order rate constant for $*[\text{Ru}(\text{dmbpy})_3]^{2+}$ with Quinones in DMF

Quenchers	K_b (M^{-1})	k_{red}
2-chloro-1,4-benzoquinone	2.5×10^4	4.124×10^5
1,4-benzoquinone	4.91×10^4	5.41×10^5
2-methyl-1,4-benzoquinone	9.77×10^4	1.21×10^6
2,6-dimethyl-1,4-benzoquinone	1.24×10^5	8.84×10^4

Determination of binding constant

The binding constant of $[\text{Ru}(\text{dmbpy})_3]^{2+}$ complex with quinones was evaluated using Benesi-Hildebrand method (Eqn. 1)

$$\frac{1}{\Delta A} = \frac{1}{K_a^{\text{abs}}} \Delta \delta ([\text{Ru}(\text{dmbpy})_3]^{2+}) + \frac{1}{\Delta \epsilon [Q]} \quad \dots(1)$$

where, ΔA is the change in the absorbance of $[\text{Ru}(\text{dmbpy})_3]^{2+}$ complex on the addition of quinone. $\Delta \epsilon$ is the difference in the molar extinction coefficient between the free and quinone bound $[\text{Ru}(\text{dmbpy})_3]^{2+}$ complex. The Benesi-Hildebrand plot of $*[\text{Ru}(\text{dmbpy})_3]^{2+}$ with 1,4-benzoquinone is shown in Fig. 6. The binding constants of $(\text{Ru}(\text{dmbpy})_3)^{2+}$ is shown in Table 1 and has the order of 10^4 M^{-1} . The first order rate constant (k_{red}) is got from the ratio of quenching rate constant k_q and the binding constant K_b .

Stern-Volmer analysis

The emission intensities of $[\text{Ru}(\text{dmbpy})_3]^{2+}$ complex are efficiently quenched in presence of quinones in DMF and are analyzed in terms of the Stern-Volmer relationship. The luminescence

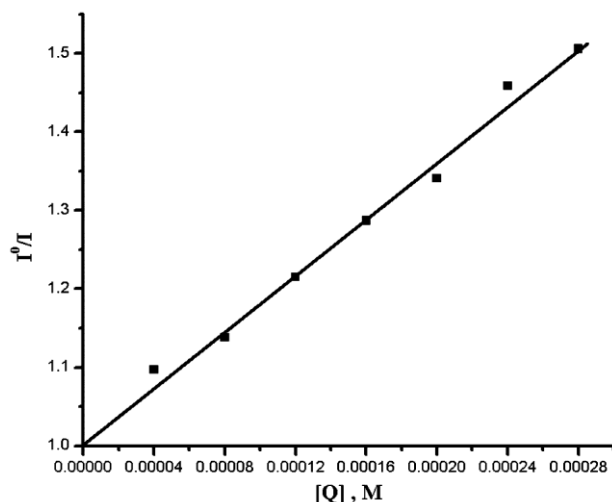


Fig. 7 — Stern–Volmer plots for the oxidative quenching of $[\text{Ru}(\text{dmbpy})_3]^{2+}$ with 2-chloro-1,4-benzoquinone in DMF.

quenching constant, k_q for the oxidative quenching of $[\text{Ru}(\text{dmbpy})_3]^{2+}$ complex with quinones used in the present study was obtained from the Stern–Volmer plot.

$$I^0/I = 1 + K_{sv}[Q] \quad \dots(2)$$

$$K_{sv} = K_q\tau \quad \dots(3)$$

Where, K_{sv} , k_q , and τ are the Stern–Volmer constant, quenching rate constant and excited state lifetime respectively. The plot of I^0/I vs $[Q]$ is a straight line with an intercept of unity in all quenching studies. The SV plot of $[\text{Ru}(\text{dmbpy})_3]^{2+}$ complex with 2-chloro-1,4-benzoquinone in DMF is displayed in Fig. 7.

Dynamics of electron transfer reactions of $[\text{Ru}(\text{dmbpy})_3]^{2+}$ with quinones

The rate of electron transfer from a donor to an acceptor in a solvent is controlled by the change in free energy (ΔG^0) of the reaction, the reorganizational energy (λ), and the electron transfer distance (d) between the donor and the acceptor. The value of k_q also depend on the nature of the substituent present in the quencher as well as the reduction potential of the quinines. The ground state oxidation potential of the Ru(II) complex in DMF is 1.320 V and that of the excited state oxidation potential of the complex is -0.78 V. The quenching rate constant k_q for the excited state electron transfer reaction of $[\text{Ru}(\text{dmbpy})_3]^{2+}$ with various quinones have been tabulated in Table 2. From the table it is inferred that

Table 2 — Luminescence quenching rate constant (k_q), reduction potential of quinones vs Ag/Ag^+ (E_{rdn}^0) and free energy changes (ΔG^0) for the oxidative quenching of $[\text{Ru}(\text{NN})_3]^{2+}$ complexes in DMF

Quencher	E_{rdn}^0 vs Ag/Ag^+ (V)	k_q (M^{-1})	ΔG^0 (eV)
2-chloro-1,4-benzoquinone	-0.322	7.005×10^{10}	-0.503
1,4-benzoquinone	-0.395	2.66×10^{10}	-0.430
2-methyl-1,4-benzoquinone	-0.402	2.3×10^{10}	-0.423
2,6-dimethyl-1,4-benzoquinone	-0.623	6.48×10^9	-0.202

all the quinones quench the excited state of $[\text{Ru}(\text{dmbpy})_3]^{2+}$ efficiently. The reduction potential of the quinones, quenching rate constant and the free energy change (ΔG) values of the quinones are also displayed in Table 2.

These values show that the value of k_q is sensitive to the reduction potential of the quinones. Quinones with high reduction potential also exhibit higher quenching rate constant values. They act as efficient quencher in the photoinduced electron transfer reaction. This is indicative for the electron transfer quenching. The lowest k_q value is observed is in accordance with highest ΔG^0 value. The value of depends on the presence of the substituent in the 4,4'-position of 1,4-benzoquinone. The presence of electron withdrawing substituent decreases the electron density and thereby increases the quenching rate constant. Thus 2-chloro-1,4-benzoquinone has higher quenching rate constant than the parent quinone 1,4-benzoquinone. It is due to the electron-withdrawing nature of the chloro group. 2,6-dimethyl-1,4-benzoquinone, which is having electron releasing group has lower quenching rate constant of $6.48 \times 10^9 \text{ M}^{-1}$.

The electron transfer distance between the donor and the acceptor also affects the rate constant. $[\text{Ru}(\text{dmbpy})_3]^{2+}$ has a radii of 7.9 Å from MM₂ molecular model calculation and the radius of quinones are in the range 2.7 Å to 4.79 Å. The electron transfer distance is the sum total radius of the donor and the acceptor. 2,6-dimethyl-1,4-benzoquinone has highest electron transfer distance. It has the least k_q value. In addition to this, Fig. 8 and Fig. 9 give the linear plot of $\text{RTln } k_q$ vs reduction potential of the quinones and $\log k_q$ vs ΔG^0 of the reaction in DMF, respectively. The Hammett plot for the reduction of quinones by $[\text{Ru}(\text{dmbpy})_3]^{2+}$ is shown in Fig. 10. This provides an additional support for the oxidative

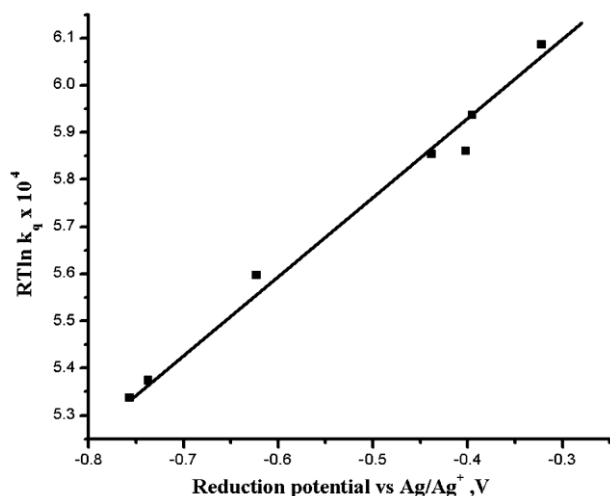


Fig. 8 — Plot of $RT \ln k_q \times 10^4$ vs reduction potential of $[\text{Ru}(\text{dmbpy})_3]^{2+}$ complex with the quinones in DMF vs Ag/Ag^+ .

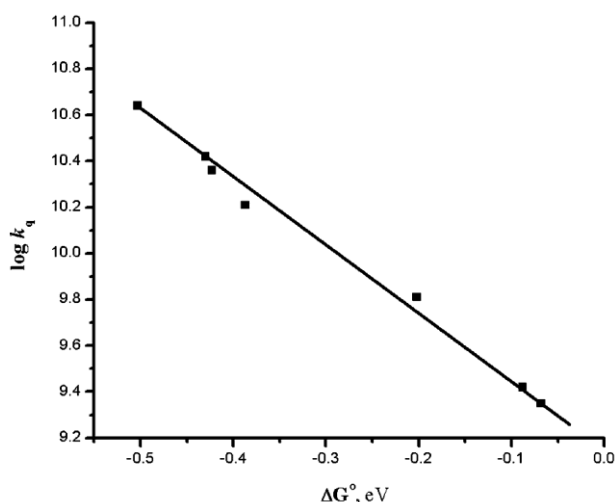


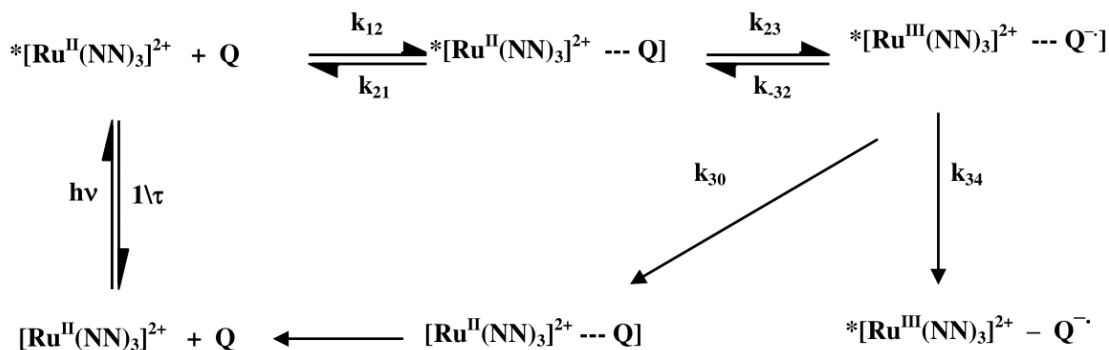
Fig. 9 — Plot of $\log k_q$ vs ΔG^0 of $[\text{Ru}(\text{dmbpy})_3]^{2+}$ complexes with quinones in DMF.

quenching of $[\text{Ru}(\text{dmbpy})_3]^{2+}$. Thus the behaviour of this redox system is depicted by the common mechanism shown in Scheme 1.

According to the Scheme, the excited state donor (Ru^{II}) and the ground state acceptor (quinone) molecules together to form an encounter complex, ($^*\text{Ru}^{\text{II}} \dots \text{Q}$). This complex then undergoes a reorganization to reach the transition state where electron transfer takes place from the donor to the acceptor to give an ion-pair species, ($\text{Ru}^{\text{III}} \dots \text{Q}^-$). For the successor complex the parameter K_{12} and K_{21} are the diffusion controlled rate constants for the formation and dissociation of the encounter complex, respectively. The parameter K_{23} and K_{32} denote the forward and reverse rate constants, respectively. Apart from the formation of precursor complex (K_{32}), the unpair state ($\text{Ru}^{\text{III}} \dots \text{Q}$), form the separated species $\text{Ru}^{\text{III}} \dots \text{Q}$ (K_{sep}) and undergo back electron transfer to form the reactants in the ground state (K_{34}).

Transient absorption spectra

To confirm the electron transfer nature of the reaction from the excited state $\text{Ru}(\text{II})$ complex to quinone, transient absorption spectrum of the reaction mixture was recorded using flash photolysis technique as shown in Fig. 11. Argon bubbled DMF solution of $[\text{Ru}(\text{dmbpy})_3]^{2+}$ complex was excited at 355 nm under laser flash photolysis. The spectrum at each time delay consists of positive, absorption maxima centered at 387 nm. 520 nm corresponds to the formation of substituted bipyridyl anion radical. In the presence of 2,3-dimethoxy-1,4-benzoquinone, a new transient species is formed around 450 nm. This broad band was assigned to the quinone anion radical¹⁵⁻¹⁹. The absorption at 450 nm is caused by the formation of quinone anion radical upon oxidative



Scheme. 1 — Schematic mechanism for the electron transfer quenching of $[\text{Ru}(\text{NN})_3]^{2+}$

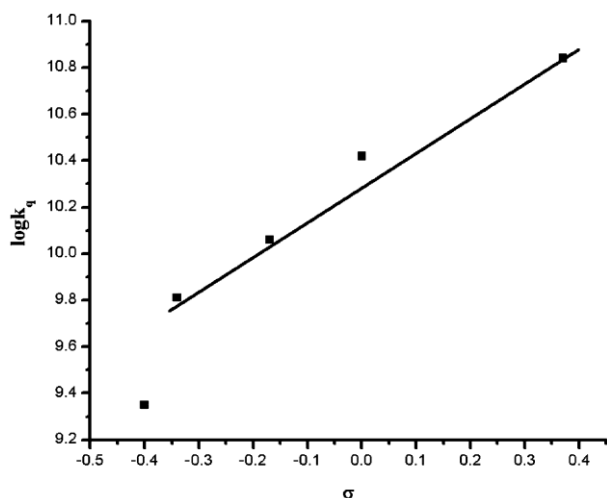


Fig. 10 — Hammett plot for the reduction of quinones by $[\text{Ru}(\text{dmbpy})_3]^{2+}$ in DMF at 298 K

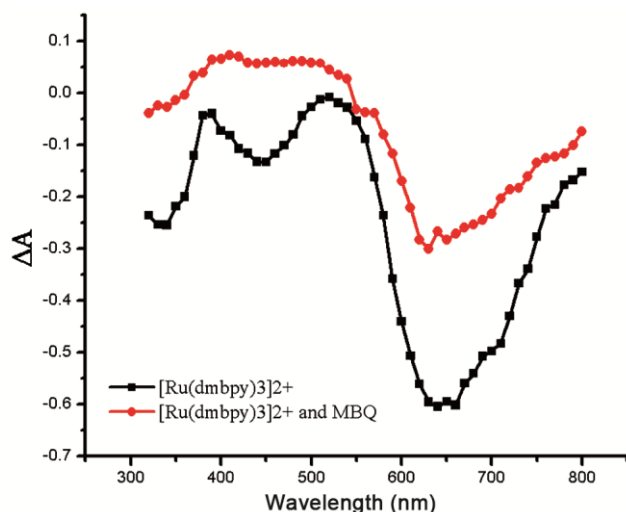


Fig. 11 — Transient absorption spectrum of complex in presence of 2,3-dimethoxy-1,4-benzoquinone.

of $^*\text{Ru}(\text{II})$ with quinone, while there is no such positive signal in this region when we have the complex alone. This transient formation confirms the electron transfer reaction

Conclusions

The photoinduced electron transfer reactions $[\text{Ru}(\text{dmbpy})_3]^{2+}$ complexes with quinones were studied by luminescence and laser flash photolysis method. The luminescence quenching data and transient absorption spectra shows that the excited state $[\text{Ru}(\text{dmbpy})_3]^{2+}$ complex undergo rapid electron transfer reactions with quinones. The

observation of quinone anion radical supports the electron transfer quenching of $^3\text{MLCT}$ excited state of $\text{Ru}(\text{II})$ complex with quinones. The quenching rate constant k_q depends on the change in the free energy value, electron transfer distance and the reduction potential of the quinones.

Supplementary Data

Supplementary data associated with this article are available in the electronic form at [http://www.niscair.res.in/jinfo/ijca/IJCA_56A_\(07\)_914-922_SupplData.pdf](http://www.niscair.res.in/jinfo/ijca/IJCA_56A_(07)_914-922_SupplData.pdf).

Acknowledgement

The authors thank Prof. P. Ramamurthy and Dr. Selvaraj of NCUFP, University of Madras, Tharamani, Chennai, for the lifetime and transient measurements.

References

- Kurreck H & Huber M, *Angew Chem Int, Ed Engl* 34 (1995) 849.
- Mandal P C, Guin Partha Sarathi & Das Saurabh, *Int J Electrochem*, (2011), 22 pages.
- Purohit N V, Rajeshire M, Shah R & Yadav P, *Der Pharmacia Sinica*, 3(2) (2012) 239.
- Masanari Hirabhar & Masayaki yagi, *Dalton Trans*, 46(12) (2017) 3787.
- Gratzel M, *Inorg Chem* 44 (2005) 6841.
- Singh V K, Giri Babu L, Vijay Kumar C, Soujanya Y, Gopal Reddy V & Yella Reddy P, *Adv OptoElectron*, (2011) 8 pages.
- Lela Duan F B, Mandal S, Stewart B, Privalov T, Liobet A & Sun L, *Nat Chem*, 4 (2012) 418.
- Brookhart M S, Concepcion J P, Harrison D P, Meyer T J, Weinberg D R, Chen Z, Chen C & Kang P, *Chem Commun*, 47 (2011) 12607.
- Ohzu S, Ishizuko T, Hirai Y, Fukuzum S & Kojima T, *Chem European J*, 19 (2013) 1563.
- Muthu Mareeswaran P, Babu E & Rajagopal S, *J Fluorescence*, 23 (2013) 997.
- Babu E, Muthu Mareeswaran P & Rajagopal S, *J Fluorescence*, 23(2013) 137.
- Karina P Morelli Frin & Rafael M de Almeida, *Photochem Photobiol Sci*, 16 (2017) 1230.
- Saha B & Stanbury D M, *Inorg Chem*, 39 (2000) 1294.
- Ramamurthy P, *Chem Edu*, 9 (1993) 56.
- Allsopp S R, Kemp T J, Reed W J & Cox A, *J Chem Soc Faraday Trans*, 1 (1978) 275.
- Baranouski L I, Lubimova O O, Makarov A A & Sizova O V, *Chem Phys Lett*, 361 (2002) 196.
- Lakowicz J R, *Principles of fluorescence spectroscopy*. Springer press, 3rd Edition, (2006)
- Roundhill D M, *Photochemistry and photophysics of neutral complexes*, Plenum press, New York, (1994)
- Balzani V, Jurin A, Venturi Campagna S & Serroni S, *Chem Rev*, 96 (1996) 759.